JOURNAL OF BACTERIOLOGY, May 1996, p. 2479–2488 Vol. 178, No. 9
0021-9193/96/$04.00+0

A Major Autolysin of *Pseudomonas aeruginosa*: Subcellular Distribution, Potential Role in Cell Growth and Division, and Secretion in Surface Membrane Vesicles

ZUSHENG LI,* ANTHONY J. CLARKE, AND TERRY J. BEVERIDGE

Center for Canadian Bacterial Diseases Network, Department of Microbiology, College of Biological Sciences, University of Guelph, Guelph, Ontario N1G 2W1, Canada

Received 20 December 1995/Accepted 21 February 1996

A 26-kDa murein hydrolase is the major autolysin of *Pseudomonas aeruginosa* PAO1, and its expression can be correlated with the growth and division of cells in both batch and synchronously growing cultures. In batch cultures, it is detected primarily during the mid-exponential growth phase, and in synchronous cultures, it is detected primarily during the cell elongation and division phases. Immunogold labeling of thin sections of *P. aeruginosa* using antibodies raised against the 26-kDa autolysin revealed that it is associated mainly with the cell envelope and in particular within the periplasm. It is also tightly bound to the peptidoglycan layer, since murein sacculi, isolated by boiling 4% sodium dodecyl sulfate treatment, could also be immunogold labeled. Since division is due to cell constriction in this *P. aeruginosa* strain (septa are rarely seen), we cannot comment on the autolysin's contribution to septation, although constriction sites were always heavily labeled. Some labeling was also found in the cytoplasm, and this was thought to be due to the de novo synthesis of the enzyme before translocation to the periplasm. Interestingly, the autolysin was also found to be associated with natural membrane vesicles which blebbed from the surface during cell growth; the enzyme is therefore part of the complex makeup of these membrane packages of secreted materials (J. L. Kadurugamuwa and T. J. Beveridge, J. Bacteriol. 177:3998–4008, 1995). The expression of these membrane vesicles was correlated with the expression of B-band lipopolysaccharide.

Both gram-positive and gram-negative bacteria possess various kinds of endogenous murein hydrolases that cleave specific covalent bonds in the peptidoglycan of the cell wall. Most of these enzymes are autolysins, since their hydrolysis of peptidoglycan results in the breakdown of the structural integrity and protective properties of the wall and eventual bacterial lysis (30). Deregulation of peptidoglycan metabolism (e.g., by addition of a β-lactam antibiotic) can activate some of these enzymes, resulting in localized peptidoglycan weakness and autolysis of cells. Autolysins are most commonly classified into four categories by their enzyme specificity, i.e., two types of glycosidases (β-*N*-acetylmuramidases [lysozymes] and β-*N*-acetylglucosaminidases), an *N*-acetylmuramoyl-L-alanine amidase, and peptidases of various specificities (27, 30). In *Escherichia coli*, three lytic transglycosylases which catalyze the cleavage of the β-1,4-glycosidic bond between *N*-acetylmuramic acid and *N*-acetylglucosamine followed by an intramolecular transglycosylation that results in the formation of 1,6-anhydromuramic acid have been identified (6, 12).

Autolysins must play important physiological roles in bacterial growth and division, since such enzyme activities are often most expressed in cultures of several species of rapidly growing bacteria under normal growth conditions. Murein hydrolases have been proposed to act as spacemaker enzymes to make room for such structures as flagella and cutting enzymes during murein expansion for cell wall turnover and for septum formation and splitting (19, 27, 28, 32); these autolysins are essential for both growth and division. Besides these functions, there is also some evidence to suggest a role for autolysins in spore formation and germination (31). Because these enzymes function as key molecules which determine growth or lysis of cells, their activity must be tightly regulated. However, the molecular details of their control and topological distribution remain largely unknown.

The murein hydrolases in *E. coli* have been extensively investigated and identified (6, 12). Of these, two are endopeptidases and three are lytic transglycosylases. Unfortunately, the autolytic systems of other gram-negative bacteria are not as well known. We have initiated studies of the autolysins of *Pseudomonas aeruginosa*, an important opportunistic pathogen that is frequently resistant to commonly used antibiotics (2, 36). Since the deregulation of the autolytic system of this pathogen is a potential strategy for clinical therapy, a more in-depth knowledge is required, especially since polycationic antibiotics such as gentamicin and amikacin are known to trigger autolysin action (16, 17, 24, 35).

Recently, a zymogram technique has been used to analyze the autolysins of several gram-negative bacteria, including those of *P. aeruginosa* (2); in this bacterium, two extracellular autolysins with molecular masses of 26 and 29 kDa have been identified and characterized (36). In the present paper, we demonstrate that the 26-kDa autolysin is the major autolysin of *P. aeruginosa* which is associated with both whole-cell extracts and culture supernatants. We also present data on its subcellular distribution, obtained by using immunogold labeling of ultrathin-sectioned cells and isolated murein sacculi. The enzyme's location suggests its role in cell growth and division, and the possible implication of its secretion in surface membrane vesicles (MVs) is discussed.

* Corresponding author. Mailing address: Department of Microbiology, College of Biological Sciences, University of Guelph, Guelph, Ontario N1G 2W1, Canada. Phone: (519) 824-4120, ext. 2533. Fax: (519) 837-1802. Electronic mail address: zli@uoguelph.ca.

MATERIALS AND METHODS

Bacteria and growth conditions. *P. aeruginosa* PAO1 and its isogenic lipopolysaccharide (LPS) mutants AK 1401 (A^+ B^-) (3), rd 7513 (A^- B^-) (23), and dps

89 (A^- B^+) (17) were used in the present study. All bacterial strains were cultured to mid-exponential growth phase (unless otherwise stated) on trypticase soy broth (TSB) (Difco Laboratories, Detroit, Mich.) at 37°C with continuous agitation on a rotary shaker at 125 rpm. Most studies were carried out with strain PAO1 except when otherwise noted.

Preparation of autolysin-containing fractions. Three different fractions from *P. aeruginosa* were prepared for analysis.

(i) Culture supernatant. A culture supernatant fraction was obtained either by precipitation of culture supernatant with 10% trichloroacetic acid as previously described (36) or by freeze-drying and dialysis. For the latter, after centrifugation of the cell culture at 5,000 × *g* for 30 min at 4°C, the culture supernatant was freeze-dried to concentrate soluble and small suspended materials. This concentrate was then resuspended in distilled water to a volume equal to that of the final suspension of the cell pellets and dialyzed against 3 liters of distilled water (in dialysis tubing having a molecular mass cutoff of 3.5 kDa) for 2 days at 4°C with changes of distilled water twice a day to remove salt. This dialyzed fraction was finally mixed with an equal volume of twofold-concentrated sodium dodecyl sulfate-polyacrylamide gel electrophoresis (SDS-PAGE) solubilization buffer (SDS-PAGE sample buffer: 62.5 mM Tris-HCl [pH 6.8], 2% SDS, 10% glycerol, 5% β-mercaptoethanol, and 0.025% bromophenol blue). The preparation was boiled for 6 min and stored at −20°C until required.

(ii) Whole-cell extract. For the whole-cell extract, the cell pellet after centrifugation of the cell culture (used for the supernatant) was suspended in SDS-PAGE sample buffer, subjected to sonication (Braun-Sonic 2000; Braun Biotech, Inc., Allentown, Pa.) for 1 min at 150 W to resuspend the pellet, boiled for 10 min, and stored at −20°C.

(iii) MVs. MVs were prepared by differential centrifugation of the culture supernatant from overnight growth culture as previously described (14).

Preparation of murein sacculi. Two liters of *P. aeruginosa* PAO1 in TSB was incubated at 37°C and 125 rpm to obtain an optical density at 600 nm (OD_{600}) of 1.0. After centrifugation at 5,000 × *g* for 30 min, the cell pellet was resuspended in distilled water, and murein sacculi were prepared by boiling cells in 4% (final concentration) SDS for 3 h as described previously (13). Murein sacculi were sonicated to homogeneity prior to incorporation into the polyacrylamide gel used in the zymogram system.

Zymogram analysis. Zymogram analysis of autolysins of *P. aeruginosa* was done as described previously (2), using the discontinuous buffer system of Laemmli (21) and an SDS–12.5% polyacrylamide separating gel containing 1% (wet weight) *P. aeruginosa* PAO1 murein sacculi in a Mini-Protein II vertical slab gel electrophoresis system (Bio-Rad Laboratories, Richmond, Calif.) (200 V, constant voltage). Prestained low-molecular-mass markers were obtained from Bio-Rad. Autolytic bands in gels were visualized as clear zones by staining the gels with 0.1% methylene blue and were then recorded by Optimas image analysis (version 4.0; BioScan, Inc., Edmonds, Wash.).

Sampling of *P. aeruginosa* at various growth phases. *P. aeruginosa* PAO1 was grown overnight in TSB at 37°C. TSB (2 liters) was inoculated with 5 ml of overnight culture and incubated at 37°C with continuous agitation on a rotary shaker at 125 rpm. Samples (10 ml) were removed from the growing culture at 1-h intervals for 12 h and at the 24-h mark. One milliliter of sample was used for measurement of the OD_{600}, and the remaining 9 ml of sample was centrifuged (15,000 × *g*, 10 min) to recover the cell pellets. For the zymogram analysis, each sample at various growth intervals was adjusted to the same OD_{600}, and the same volume of these samples was subjected to centrifugation to recover the cell pellets, which were subsequently boiled in SDS-PAGE sample buffer.

Synchronized growth of *P. aeruginosa*. *P. aeruginosa* PAO1 (100 ml) was grown overnight in TSB, and cells were synchronized by the membrane elution (or baby machine) technique (10). Type GS, 90-mm-diameter, 0.22-μm-pore-size nitrocellulose membrane filters (Millipore Corp., Bedford, Mass.) were used in this study. One hundred milliliters of fresh TSB was passed through each membrane, and this was followed with 100 ml of bacterial culture by use of a peristaltic pump operated at a rate of 5 ml/min. To avoid drying the cells, filtration was stopped when approximately 5 ml of culture medium still remained above the membrane. The filter holder was then inverted, and the new upper portion of the holder was aseptically immersed in new TSB. Fresh medium was then pumped through the membrane at a rate of 4 ml/min for 15 min to remove unattached cells, and the rate was then reduced to 2.5 ml/min.

Five-milliliter samples of the effluent were collected, cultured in 100 ml of fresh TSB, and incubated at 37°C with continuous agitation on a rotary shaker at 125 rpm. These cells remained synchronous for at least three generations, with a generation time of approximately 50 min. Therefore, for subsequent experiments, a 0.5-ml portion was removed from the culture at 5-min intervals, immediately mixed with 25 μl of formaldehyde (5%, final concentration), and stored at 4°C for the purpose of cell counting. In addition, a 4-ml portion was simultaneously removed from the culture at 5-min intervals starting at the 40-min incubation point and immediately centrifuged for 5 min at 15,000 × *g* to pellet the cells. The pellets were kept frozen at −20°C until analyses were performed.

Cell counts. Samples (0.1 ml) of culture harvested at each interval were diluted with 20 ml of isotonic diluent (Fisher Scientific Co., Toronto, Canada) in a vial, and cells were counted three times (for averaging) with a model ZM Coulter Counter (Coulter Electronics of Canada, Ltd., Burlington, Ontario, Canada) equipped with a 30-μm-diameter orifice.

Isolation of the 26-kDa autolysin. The 26-kDa autolysin was prepared from a whole-cell extract of *P. aeruginosa* PAO1, and the proteins were separated by SDS-PAGE in 12.5% polyacrylamide separating gels. The gels were run (as described above) until the desired protein reached the bottom of the gels. The band was cut out and electroeluted with a Mini-Protein II electroelution apparatus (Bio-Rad) according to the manufacturer's instructions. This was repeated until enough protein for antibody production was obtained. The protein was subsequently dialyzed in distilled water, and trace amounts of contaminating LPS were removed by three passages through an AffinityPak detoxi-gel column (Pierce, Rockford, Ill.) according to the manufacturer's instructions. The isolated protein was confirmed to be the 26-kDa autolysin by zymogram analysis.

Production of monospecific polyclonal antibodies against the 26-kDa autolysin. Antibodies against the 26-kDa autolysin were produced in an adult New Zealand White rabbit. Since sera from conventional and specific-pathogen-free rabbits contained antibodies against *P. aeruginosa* (presumably because of the wide spread of this microorganism in the environment), 20 serum samples from conventional rabbits were screened by Western blotting (immunoblotting) against whole-cell extracts, and the rabbit with the lowest background level was chosen for the study. This animal was injected once a week for 5 weeks with approximately 800 μg of protein emulsified in 3 ml of Freund's incomplete adjuvant. The animal received 0.2 and 0.5 ml of antigen by subcutaneous injection during the first and second weeks, respectively, and 1.0 ml of antigen by intramascular injection in the subsequent weeks. When positive results were obtained by Western blotting after a small amount of serum, obtained 1 week after the fifth injection, was tested against both whole-cell extracts and the isolated 26-kDa autolysin, the rabbit was bled by cardiac puncture and the serum was collected. This antiserum was further adsorbed with a nitrocellulose membrane containing the whole-cell proteins and LPS (see "Western blotting" below) but not the 26-kDa autolysin. Control preimmune serum was obtained before the first injection.

Western blotting. Western blotting was performed by the method of Towbin et al. (33). The samples separated by electrophoresis were transferred (Mini-Protein II transfer system; Bio-Rad) to nitrocellulose membrane blotting paper (pore size, 0.2 μm; Bio-Rad) for 1 h at 100 V. The membrane was blocked with 2% skim milk in Tris-buffered saline (10 mM Tris [pH 7.4], 150 mM NaCl) for 1 h and incubated with diluted antiserum in the blocking solution overnight at 4°C. The membrane was then washed in Tris-buffered saline, and bound antibodies were detected with horseradish peroxidase-conjugated goat anti-rabbit immunoglobulin G (Bio-Rad) by using 4-chloro-1-naphthol as the chromogenic substrate.

Electron microscopy. (i) Conventional embedding. Cells were prepared from mid-exponential-growth-phase cultures by centrifuging the cultures and washing them once with 20 mM sodium phosphate-buffered saline (PBS), pH 7.2. These preparations and those of murein sacculi were enrobed in 2% (wt/vol) agarose and fixed for 1 h at 4°C with a solution containing 0.1% (vol/vol) glutaraldehyde and 2% (vol/vol) formaldehyde in 100 mM HEPES (*N*-2-hydroxyethylpiperazine-*N*′-2-ethanesulfonic acid) (Sigma) buffer (pH 6.8). Samples were washed twice with HEPES buffer and once with distilled water, incubated in 2% (wt/vol) aqueous uranyl acetate for 45 min at 4°C, and dehydrated in 75 and 90% (vol/vol) ethanol for 15 min each at 4°C and in 100% ethanol for 15 min at 4°C twice. After infiltration with 50% (vol/vol) LR White (Marivac, Ltd., Halifax, Canada) for 4 h and 100% LR White overnight, samples were embedded in 100% LR White for 2 h at 60°C for polymerization and thin-sectioned with a Reichert OM U4 Ultracut ultramicrotome. Sections were collected on nickel grids (mesh size, 400 μm) covered with a carbon- and Formvar-coated film.

(ii) Immunogold labeling. For immunogold labeling of whole mounts of sacculi, the grids were floated on sacculus preparations for 10 min at room temperature to adsorb the sacculi to the grid and air dried. For both sacculi and thin sections, the sample grids were blocked with 0.5% glycine in PBS and with 1% bovine serum albumin in PBS (each for 30 min), incubated for 1 h with suitably diluted antiserum, and washed five times with distilled water. The grids were then incubated for 30 min with protein A-gold (10-nm diameter; Sigma), washed five times as before, and stained with 1% (wt/vol) aqueous uranyl acetate for 10 min. The sample grids were examined with a transmission electron microscope (Philips EM300) operated under standard conditions at 60 kV with the anticontamination device in place.

RESULTS

Major autolysins of *P. aeruginosa*. The autolysin profile of *P. aeruginosa* PAO1 was examined by zymogram analysis and is shown in Fig. 1A. Two major autolysin bands were present in both whole-cell extract (Fig. 1A, lane 1) and culture supernatant (lane 2), and they had molecular masses of 26 and 29 kDa. These two autolysins were apparently the same enzymes described as extracellular autolysins in a previous study (36). The 26-kDa band was the most pronounced clear zone of autolytic activity, which was visible in gels even prior to staining with methylene blue. The 29-kDa band was clearly present but far

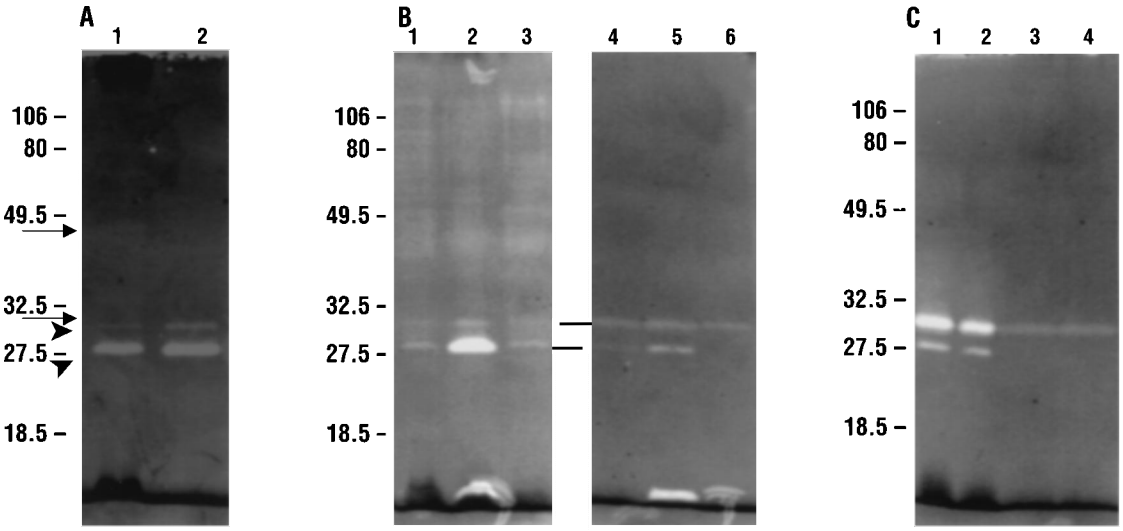

FIG. 1. Autolysin profile of *P. aeruginosa* by renaturing SDS-PAGE using a 12.5% polyacrylamide gel containing 1% (wet weight) homologous murein sacculi. (A) Wild-type PAO1 profile. Lane 1, whole-cell preparation; lane 2, culture supernatant. (B) Profile of LPS mutants. Lanes 1 and 4, strain AK 1401 (A^+ B^-) whole-cell extract and culture supernatant, respectively; lanes 2 and 5, strain dps 89 (A^- B^+) whole-cell extract and culture supernatant, respectively; lanes 3 and 6, strain rd 7513 (A^- B^-) whole-cell extract and culture supernatant, respectively. (C) Autolysin activities of MVs. Lanes 1 and 2, MVs isolated from wild-type cells and those treated with gentamicin, respectively; lanes 3 and 4, high-speed centrifugation supernatants from wild-type cells and gentamicin-treated cells, respectively. Each lane in each panel contains approximately 20 to 30 μg of total protein. Prestained low-molecular-mass markers (in kilodaltons) are indicated to the left of each gel. Arrows and arrowheads indicate 26-, 29-, 31-, and 46-kDa autolytic bands.

less pronounced than the 26-kDa band. These two bands were always detected consistently in all samples of whole-cell extracts or culture supernatants in all independent experiments. Other minor autolytic bands were present frequently in whole-cell extracts but varied between independent experiments. Of these, autolytic bands with molecular masses of 46 and 31 kDa were most often detected.

Since gentamicin induces autolytic activity in whole cells, especially in those containing B-band LPS (2, 24), we attempted to determine if there was any correlation between expression of A-band and B-band LPSs and concentrations of autolysins. To do this, autolysin profiles of isogenic LPS mutant strains (AK 1401 [A^+ B^-], dps 89 [A^- B^+], and rd 7513 [A^- B^-]) were examined (Fig. 1B). The activities of the 26- and 29-kDa autolysins were detected in whole-cell extracts of all LPS mutants (Fig. 1B, lanes 1 through 3), with the most pronounced activity of the 26-kDa autolysin seen in strain dps 89. Different autolysin profiles were also detected in the culture supernatants from these mutants. In these, while the activity of the 29-kDa autolysin was detected in all mutants, the activity of the 26-kDa autolysin detected was as follows: full activity in dps 89 (Fig. 1B, lane 5), trace activity in AK 1401 (lane 4), and no activity in rd 7513 (lane 6). In addition, another autolytic band with a very low molecular mass (<18 kDa) was detected in both the whole-cell extract (Fig. 1B, lane 2) and the culture supernatant (lane 5) of strain dps 89.

It has been shown previously that *P. aeruginosa* naturally releases MVs into the culture supernatant during normal growth, and the number of these vesicles increases when cells are treated with gentamicin (14, 17). It is possible that autolysins present in culture supernatants may be secreted, at least in part, through MVs. MVs were purified from untreated cells and gentamicin-exposed cells as previously described (14). Both MVs and the remaining supernatants were retained for renaturing SDS-PAGE analysis (Fig. 1C). We found that the major activity of both 29- and 26-kDa autolysins was recovered in MV preparations (Fig. 1C, lanes 1 and 2) but not in the supernatants (lanes 3 and 4). In this case, however, the 29-kDa autolytic band was more prominent than the 26-kDa band, possibly in part because of preparation of MVs from late-exponential-phase or stationary-phase cultures. Very weak activity of the 29-kDa autolysin, but not of the 26-kDa autolysin,

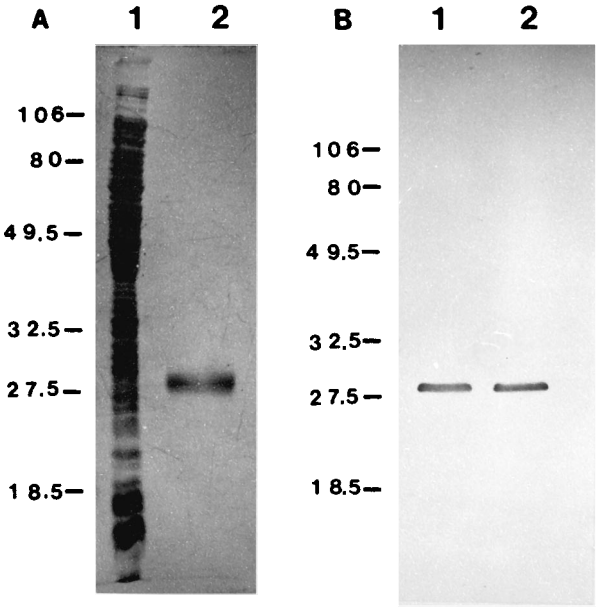

FIG. 2. Specificity of the polyclonal rabbit antiserum against the *P. aeruginosa* PAO1 26-kDa autolysin. Results of SDS-PAGE (A) and Western blotting (B) with antiserum against the 26-kDa autolysin are shown. Lanes 1, whole-cell extract (30 and 15 μg of total protein in panels A and B, respectively); lanes 2, the isolated 26-kDa autolysin from PAO1 (6 and 3 μg of protein in panels A and B, respectively). Prestained low-molecular-mass markers (in kilodaltons) are indicated to the left of each gel.

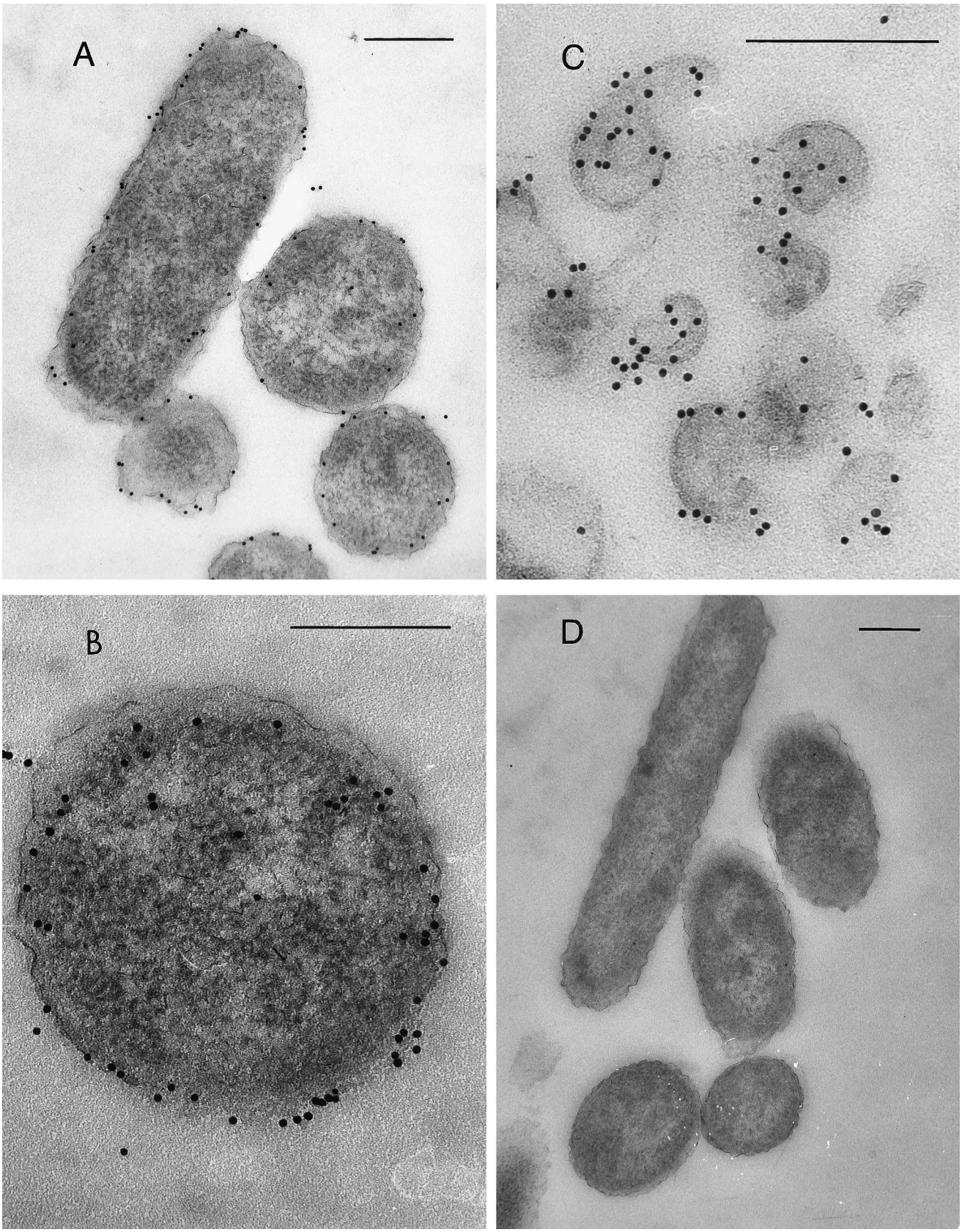

FIG. 3. Immunogold labeling of the 26-kDa autolysin in ultrathin sections of *P. aeruginosa* PAO1. Sections were immunolabeled with antiserum against the 26-kDa autolysin, showing predominant labeling of the cell envelope, especially in the periplasmic space (A), slight labeling of the cytoplasm (B), and abundant labeling of MVs (C). A control is also shown (D). Bars, 200 nm.

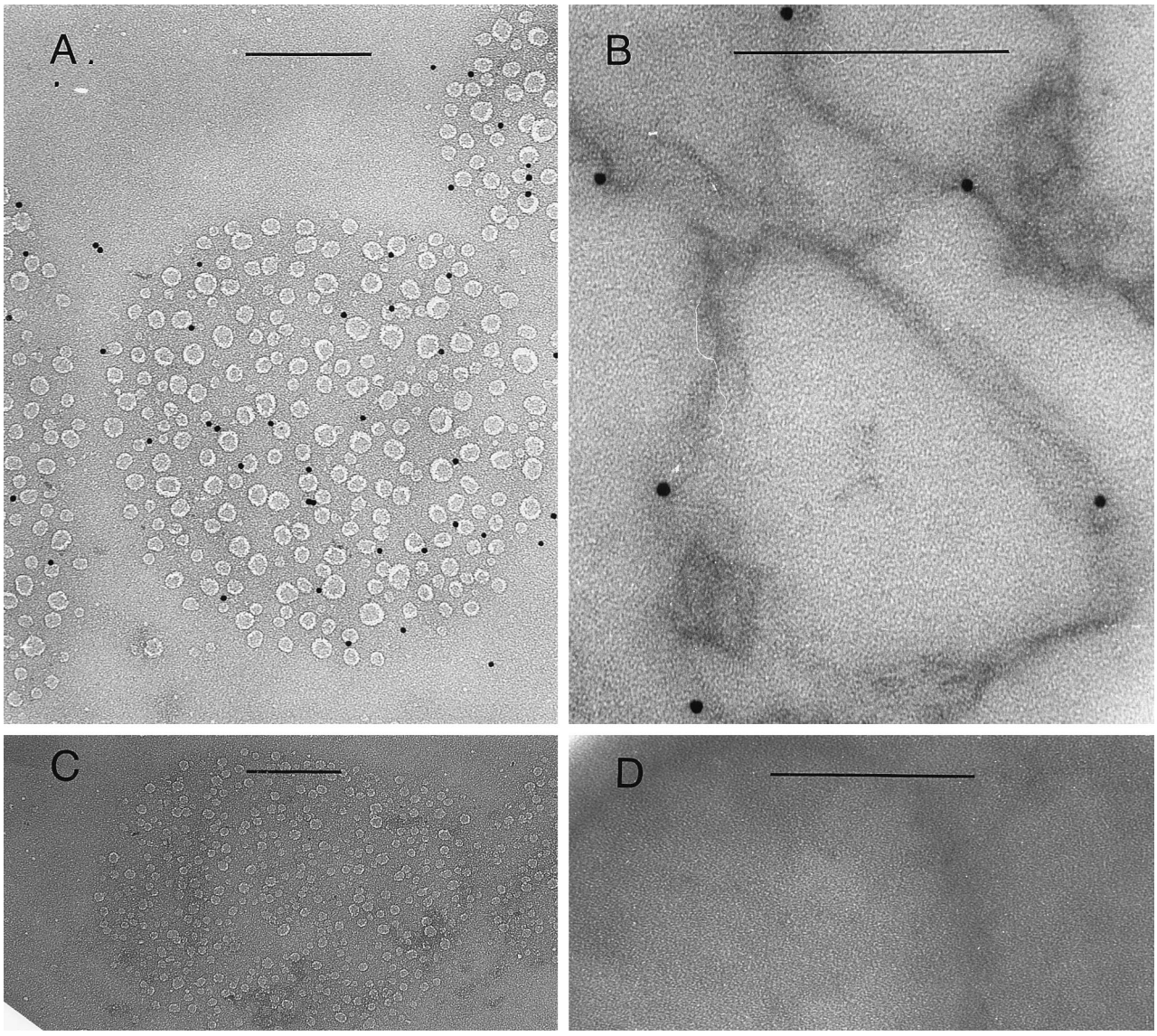

FIG. 4. Binding of the 26-kDa autolysin to isolated murein sacculi. (A) Immunogold labeling of *P. aeruginosa* PAO1 murein sacculi with anti-26-kDa autolysin antibodies; note that electron-transparent patches associated with the sacculi are due to the interaction of the electron beam with residual SDS attached to the sacculi. (B) Immunogold labeling with anti-26-kDa-autolysin antibodies on thin-sectioned PAO1 murein sacculi. (C and D) Samples similar to those shown in panels A and B, respectively, but incubated with preimmune serum as controls. Bars, 200 nm.

was detected in the remaining supernatants (lanes 3 and 4). In addition, faint activities of two or three minor autolysins were also detected in MV preparations (Fig. 1C, lanes 1 and 2). These observations thus account for the increase in autolytic activity associated with culture supernatants treated with Triton X-100 as noted in a previous study (36).

Specificity of the polyclonal rabbit antiserum against the 26-kDa major autolysin. The 26-kDa autolysin isolated from whole-cell extracts by SDS-PAGE was found to be homogeneous as revealed by Coomassie blue staining (Fig. 2A, lane 2) in comparison with the entire protein profile from whole cells (lane 1). Antibodies raised against the 26-kDa autolysin were tested by Western blotting, and no nonspecific cross-reactivity with other proteins, including the 29-kDa enzyme, in whole-cell extracts could be detected (Fig. 2B, lanes 1 and 2). Furthermore, thin-sectioned cells were specifically labeled with the specific antiserum, whereas the same cells were virtually unlabeled with the preimmune serum (described below).

Localization of the 26-kDa autolysin on ultrathin sections. Preliminary experiments indicated that although cellular ultrastructure in ultrathin sections prepared by freeze-substitution was more effectively preserved than those prepared by conventional embedding, the antigenicity of the 26-kDa autolysin was largely destroyed by the osmium tetroxide used during the substitution process (8). Therefore, immunogold labeling experiments were performed with ultrathin sections prepared by conventional embedding as detailed in Materials and Methods. The effectiveness of antigenic preservation of the 26-kDa autolysin in these preparations was excellent, as revealed by the number of gold particles found on the sections. About 40 to 200 immunogold particles were typically seen on

each longitudinally sectioned cell, and 15 to 60 were seen on each cross-sectioned cell (Fig. 3A and B).

Differentiation of the immunolabel into different cellular compartments, such as outer membrane, plasma (cytoplasmic) membrane, and periplasmic space, was difficult because of the size and orientation of the antigen-antibody-protein A-gold complex. Nevertheless, electron micrographs showed that some of the immunolabel appeared to be associated with both outer and plasma membranes, with only a small number of particles in the cytoplasm (Fig. 3A and B). Most label in the cell envelope seemed to be associated with the periplasm (Fig. 3A and B). In addition, membrane vesicles were also labeled with the anti-26-kDa-autolysin serum (Fig. 3C).

Binding of the 26-kDa autolysin to isolated murein sacculi. Since the peptidoglycan layer is the major periplasmic structure in the thin-sectioned cells, we probed the 26-kDa autolysin for its association with murein sacculi. Immunogold labeling showed that the enzyme was indeed strongly associated with murein sacculi and that its antigenicity had been retained even after boiling in 4% SDS for 3 h during preparation of the sacculi. This is analogous to the situation of the lytic transglycosylase of *E. coli* (34). About 30 to 50 gold particles were found on each sacculus (Fig. 4A). This labeling was also apparent when thin sections of the murein sacculi were treated with the immunogold (Fig. 4B). There was no labeling with preimmune serum (Fig. 4C and D). Again, because the peptidoglycan layer is so thin, precise determination of the location of the 26-kDa autolysin on ultrathin-sectioned sacculi was difficult. As shown in Fig. 4B, it appeared that more particles labeled the outer face than the inner face of sacculi.

Autolysin activities in *P. aeruginosa* during growth. To determine if a correlation between autolysins and growth phase exists, a growth curve was generated from a culture from which samples were removed at 1-h intervals (Fig. 5A). The autolytic activities were detected by renaturing SDS-PAGE, and two major autolysins were detected throughout growth (Fig. 5B). The cell-associated 26-kDa autolysin gradually increased during early exponential growth phase and reached a maximum at mid-exponential growth phase; thereafter, it declined. The activity of the 29-kDa autolysin was clearly detected during mid-exponential growth phase and stationary phase. Of several other autolytic bands detected, the activity of the 46- and 31-kDa bands was most obvious, and this did not vary during the different growth phases (Fig. 5B). It is important to recognize that the difference in autolytic activities in these samples was not due to a difference in total cell mass, since cell masses were adjusted to the same level before zymograms were attempted. Therefore, these are real differences seen during growth. When these samples from the various growth phases were Western blotted with 26-kDa-autolysin antiserum, the reactions were always positive (Fig. 5C) and the intensity of the blots over time was relatively constant. From comparison of Fig. 5B and C, it was apparent that the activity of the enzyme must be regulated during growth so that exponential-growth-phase cultures had more activity of the 26-kDa autolysin.

Synchronization of *P. aeruginosa* PAO1 cells and expression of the 26-kDa major autolysin. To confirm the growth relationship of the 26-kDa autolysin, we analyzed synchronized cultures. By the membrane elution approach, well-synchronized cells were obtained, with synchrony lasting at least three generations; these cells had a generation time of approximately 50 min. A synchrony curve was established by plotting cell number (milliliters $\times 10^6$) as a function of incubation time after the cells were eluted from the membrane and cultured in fresh medium (Fig. 6A). The morphological characteristics and size distribution of synchronized *P. aeruginosa* PAO1 cells are

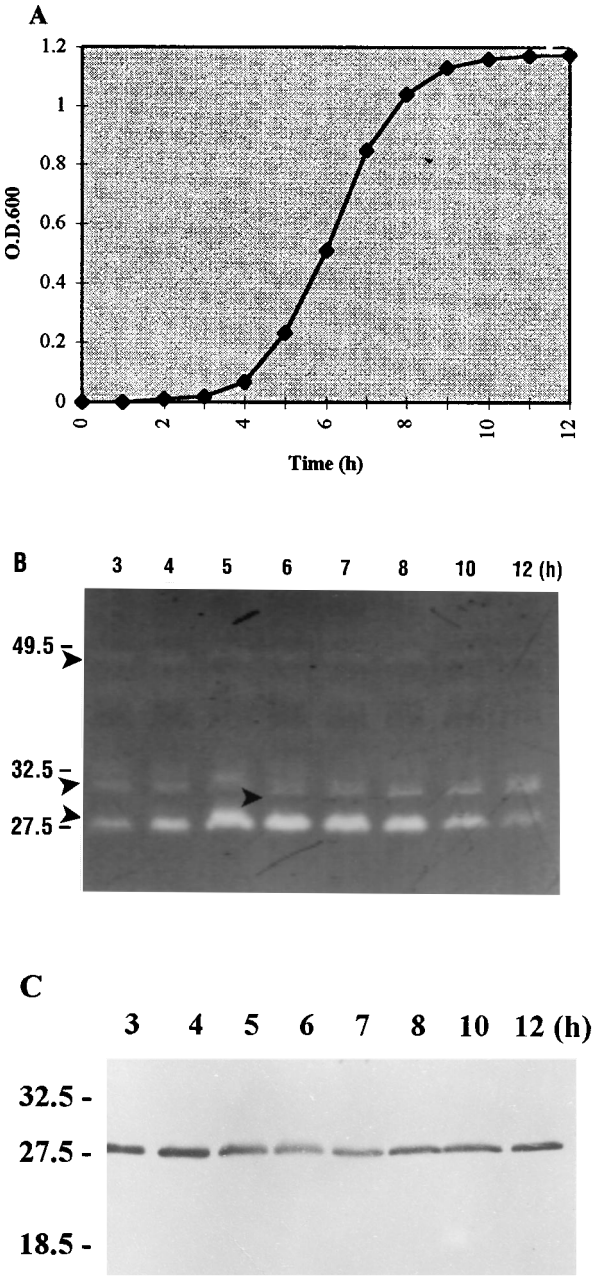

FIG. 5. Autolysin profiles of *P. aeruginosa* PAO1 during various phases of growth. (A) Growth curve of PAO1, plotted as OD_{600} versus time. (B) Zymogram analysis of PAO1 autolysins in whole-cell extracts from cultures collected at the indicated intervals. (C) Western blot analysis, using antibodies against the 26-kDa enzyme, of PAO1 autolysins in whole-cell extracts from cultures collected at the indicated intervals. Each lane in panels B and C contains approximately 30 and 15 μg of total proteins, respectively. Prestained low-molecular-mass markers (in kilodaltons) are indicated on the left. Arrowheads indicate 26-, 29-, 31-, and 46-kDa autolytic bands.

presented in Fig. 6B, as derived from both optical and electron microscopy. The new cells at the begining of the second generation (50-min fraction) were smallest (cell length [mean ± standard deviation], 1.53 ± 0.09 μm), gradually growing (60- and 70-min fractions) until a maximal size (cell length, 2.98 ± 0.13 μm) was reached (80-min fraction), which was about twice the size of the new cells as they divided (100-min fraction). The

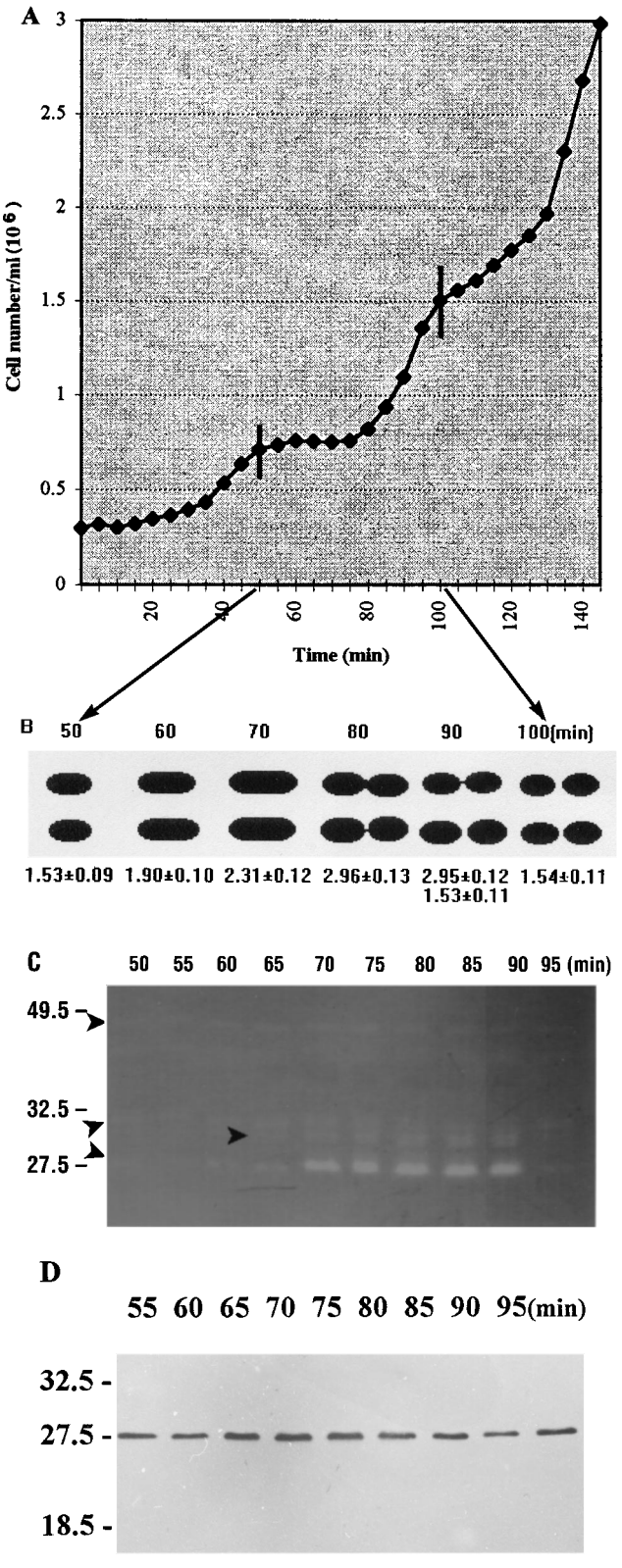

FIG. 6. Analysis of autolysins of *P. aeruginosa* PAO1 from the cell cycle of synchronized cultures. (A) Cell cycle curve for PAO1, plotted as cell number versus incubation time. (B) Morphological characteristics and size distribution (mean cell lengths [in micrometers] ± standard deviations) of cells from cultures collected at the indicated intervals. (C) Zymogram analysis of PAO1 autolysins in whole-cell extracts from synchronous cultures collected at the indicated intervals. (D) Western blot analysis, using antibodies against the 26-kDa enzyme, of PAO1 autolysins in whole-cell extracts from synchronous cultures collected at the indicated intervals. Each lane in panels C and D contains approximately 30 and 15 μg of total proteins, respectively. Prestained low-molecular-mass markers (in kilodaltons) are indicated on the left. Arrowheads indicate 26-, 29-, 31-, and 46-kDa autolytic bands.

activities of autolysins in cells at various stages of the cell cycle in the synchronized culture were examined by zymogram analysis (Fig. 6C). Again, the 26-kDa autolysin was the major autolysin detected in all stages of the cell cycle, whereas the activity of the 29-kDa autolysin was present only in the later stages of the cell cycle. The activity of the 26-kDa autolysin was fairly weak during the early growth stage (50-min fraction) but increased during cell elongation (55- to 70-min fractions), reaching a maximum just prior to or at the begining of cell separation (presumably during cell septum-constriction formation and splitting) (75- to 85-min fractions). Activity declined to lower levels during the final stage of cell separation (95-min fraction). Similar to the results of the previous growth experiments, several other minor autolytic bands were detected, with the 46- and 31-kDa autolytic bands being visible but their activities unchanging during the cell cycle (Fig. 6C). The 26-kDa autolysin reacted uniformly with the specific antiserum in all samples from different stages of growth (Fig. 6D). No statistically distinct difference in the number of immunogold particles bound to sectioned cells was found in these samples from different growth stages. Immunogold labeling of dividing cells with the specific anti-26-kDa-autolysin serum showed that immunogold particles were evenly distributed along the cell envelope, and, although constriction sites were always well labeled, no preferential label was found in these regions of the cell (Fig. 7).

DISCUSSION

Without controlled autolytic activity on the murein sacculus of peptidoglycan-bearing bacteria, there can be neither cell growth nor division. New polymeric substances must be incorporated into the sacculus, and (usually) old material must be discarded or recycled in such a way that the net result is the expansion of the peptidoglycan sacculus (i.e., cell growth) (30). Entirely new material is laid down at septal regions so that ingrowth of the sacculus bisects the mother cell. The two daughter cells then repeat the growth and division cycles. For some gram-negative bacteria, such as *P. aeruginosa*, it is exceedingly difficult to preserve septa for electron microscopy unless certain bacterial strains or fixation procedures are used (7); constrictive division sites are more commonly seen (4).

Two autolysins, the 29- and 26-kDa enzymes, had previously been shown to be the major extracellular murein hydrolases of *P. aeruginosa* and were also thought to be associated with the cell envelope (36). The present study is more precise and definitive; it confirms their presence in culture supernatants but also clearly demonstrates their tight association with the cell envelope, particularly with the peptidoglycan layer. Isolation of peptidoglycan by biochemical means in the previous study (36) may not have been able to entirely release the enzymes from the peptidoglycan meshwork, and it is also possible that the total activity of the extracted enzymes was not detectable. Furthermore, the 26-kDa autolysin was the dominant enzyme, and its expression was dependent on the cell cycle. Another study by our group (2) also used the zymogram technique and detected a total of 18 autolytic bands. In that study, *P. aeruginosa* was cultured in rich brain heart infusion and was harvested at the stationary growth phase. Our present

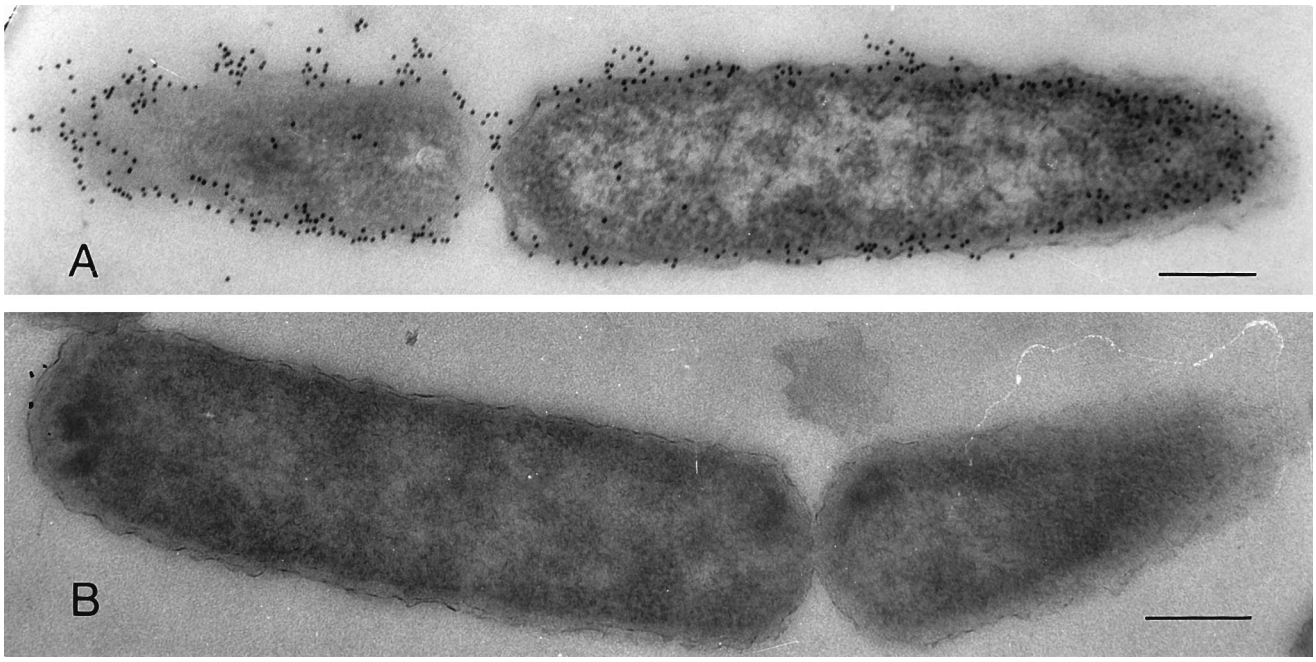

FIG. 7. Immunogold labeling with anti-26-kDa-autolysin antibodies of a thin-sectioned cell during cell separation in synchronized growth cultures. (B) A similar cell incubated with preimmune serum as a control. Bars, 200 nm.

study revealed that all autolysins were relatively minor at this growth phase. It is apparent that growth medium and growth phase can be important aspects for these types of studies. In fact, the major 26-kDa autolysin could not be detected as a pronounced clear zone in zymogram gels in either culture supernatant (36) or whole-cell extracts (this study) unless exponential-growth-phase samples were used.

P. aeruginosa can express two types of LPS, known as A-band (the antigenic conserved form) and B-band (the serotype-specific form) LPSs (25, 26). Examination of the activities of autolysins in our isogenic LPS mutants revealed that the 26- and 29-kDa autolysins were present in all whole-cell extracts. However, two anomalies were observed. First, an additional autolytic band with a molecular mass of <18 kDa was detected in both the supernatant and the whole-cell extract of the A^- B^+ mutant. The expression of this autolysin did not seem to be associated with the depleted expression of the A-band LPS, since the A^- B^- double mutant did not express this autolysin. Second, the activity of the 26-kDa enzyme was not detected in the A^- B^- supernatant and only barely detected in the A^+ B^- supernatant. Neither of these strains expressed B-band LPS. However, the full activity of the 26-kDa autolysin was detected in A^- B^+ and wild-type strains. This coincidence suggests that secretion of the active 26-kDa autolysin into the growth medium was associated with expression of the B-band LPS. A major proportion of the secreted autolysin was associated with the MVs which blebbed from the cells during growth (Fig. 1C) (15). Interestingly, B-band LPS is the only type of LPS that can be detected in these natural MVs (14). B-band LPS is very different from the A-band variety. The former has long O side chains extending up to ~40 nm from the outer membrane (22) consisting of a trisaccharide (two uronic acid derivatives in the β-D-manno configuration plus one *N*-acetyl-D-fucosame [18]) which is highly charged at a neutral pH. The inner portion of the B-band LPS molecule is highly phosphorylated (~12 phosphate groups) and possesses three carboxylate groups on ketodeoxyoctonate residues (37); each of these ionizable groups would add to the molecule's electronegativity. Clearly, external counterions are required to counteract and neutralize these charges, but the extensive length of the O side chain and core region may make this difficult. If so, then the electronegative groups on the upper portions of adjacent B-band LPS molecules would repel one another, compressing the lower fatty acid chains in the hydrophobic region of the membrane. This would force this particular region of the outer membrane into a greater curvature than normal and would initiate bleb formation; thermodynamically, this tendency towards a high degree of curvature would tear a small MV from the surface (15). During the formation of such a vesicle, underlying periplasmic components (including autolysins) would be trapped within the bleb.

Bleb formation is less likely to occur with A-band LPS because it has neutral and smaller O side chains consisting of α1-2- and α1-3-linked D-rhamnose (1) and little phosphate. Since there would be little charge-charge interaction, electrostatic repulsion of the upper portions of the molecule would be minimal and greater surface curvatures of the outer membrane would be avoided. In fact, this may be one of the functions of A-band LPS in the outer membrane, i.e., to dampen the tendency of B-band LPS to induce bleb formation. Mixtures of the two varieties of LPS would be more thermodynomically stable at low levels of curvature in lipid bilayers and would encourage those curvatures that are required in an outer membrane as it surrounds the cell. Possibly, relatively rare regions of the outer membrane contain high concentrations of B-band LPS, and these would be more prone to bleb. If the bacterium could somehow control the number and location of these particular B-band outer membrane regions, it may also be able to control the quantity and periplasmic contents of naturally produced MVs.

Surface-active antibiotics such as amikacin, gentamicin, or polymyxin can induce greater numbers of membrane blebs in *P. aeruginosa* (20, 24, 35), and these (at least with gentamicin) contain some A-band LPS (14). They are cationic antibiotics

which compete with and displace essential Mg^{2+} and Ca^{2+} in the outer membrane (24). In this case, the antibiotics would further destabilize the LPS (primarily B-band LPS), increase bleb formation, and weaken the cell envelope (16, 17). The interaction between antibiotic and outer membrane would be so rapid and dramatic that small quantities of A-band LPS could be trapped with the B-band variety as vesicles are formed. Gentamicin-induced MVs also contain the autolysins (Fig. 1C and reference 15).

The existence of autolysin in natural MVs of *P. aeruginosa* leads to an interesting speculation. This potent murein hydrolase could be used to hydrolyze the peptidoglycan of other, neighboring bacteria so that they lyse and provide nourishment for the host cell; these then could be considered predatory MVs. Because the autolysin is packaged into small bilayered vesicles which would adhere to and fuse into gram-negative surfaces, the enzyme would be liberated into the foreign periplasm, where it could hydrolyze the peptidoglycan (15). Since it is a *P. aeruginosa* autolysin, it should be most active on A1γ peptidoglycan, which is the chemotype of most gram-negative bacteria (29). Although these vesicles would also fuse to neighboring *P. aeruginosa* cells of the same strain, the autolysin would be recognized and therefore regulated, and hydrolysis of the peptidoglycan would not ensue.

It is interesting that the greatest autolysin activity present in both culture supernatant (36) and whole-cell extracts (this study) in *P. aeruginosa* was seen at the mid-exponential growth phase of cultures. Clearly, this is when the cells of the culture are actively growing and dividing and when they have the shortest doubling time. It is also during this period that the bacterium's metabolic activity is greatest and that the demands for carbon, nitrogen, phosphorus, and other nutrients are the greatest. Obviously, when the cells are growing in a nutrient-rich, laboratory broth culture, these demands are provided for. However, under more-natural conditions in which the bacterium is competing with diverse microbial consortia, the lean environmental conditions could pose a problem. In this context, it may be advantageous for an increased number of predatory MVs to be discharged to increase the nutrient supply. Therefore, there would be a peak cellular demand during growth not only for autolysins to be used in cell elongation and division, but also for predatory vesicles for nutrient supply.

The activity of the 26-kDa autolysin varied at different growth stages in the cell cycle during the synchronous growth experiment. Our T period for *P. aeruginosa* approaches the values that Helmstetter (9) derived for some *E. coli* strains; i.e., $T_{E.\ coli}$ = 10 to 14 min with generation times of 25 to 62 min, whereas $T_{P.\ aeruginosa}$ = ~13 min with a generation time of 50 min. In *P. aeruginosa*, actual physical separation of the two daughter cells during the second generation started at ~85 min and finished at ~98 min (Fig. 6A). Maximal expression of the 26-kDa autolysin occurred in the 70- to 90-min fractions (Fig. 6C), suggesting that the enzyme plays an important role in cell elongation and division. To this end, we performed immunogold labeling of dividing cells with specific antibodies. The autolysin is found all around the cell periphery (Fig. 7) and is presumably involved in cell elongation. In at least two other bacterial systems, the amidases of *Bacillus subtilis* and *Streptococcus pneumoniae*, the enzymes were found to be located at the site of cell division, i.e., in the septa of dividing cells (5, 11). However, we were unable to visualize preferential association of the enzyme with the septal region of *P. aeruginosa* by immunoelectron microscopy. We believe that this is primarily because of a technical problem. *B. subtilis* and *S. pneumoniae* are gram-positive bacteria, and their septa can be more readily preserved by conventional embedding techniques than can those of gram-negative bacteria (4). In gram-negative bacteria, constrictive division sites and not septa are frequently seen. In fact, septa in *P. aeruginosa* have only rarely been preserved and require unusual aldehyde fixatives (e.g., crotonaldehyde) and osmium tetroxide (7). Even though more-modern techniques (such as freeze-substitution) preserve septa better, osmium tetroxide must still be used to stabilize structure (8), but this reagent destroys antigenicity. The problem, then, is to somehow preserve the structure of septa in *P. aeruginosa* without at the same time destroying the antigenicity of the 26-kDa autolysin. So far, we have not succeeded in overcoming this obstacle. In Fig. 7, only constrictive division sites are seen, and even though there are high concentrations of the immunolabel at these sites, we cannot make any accurate statements about the involvement of the autolysin in septum formation and cell splitting.

ACKNOWLEDGMENTS

We acknowledge the technical assistance of B. Harris, D. Moyles, and A. Saxena of our laboratory. We thank J. Kadurugamuwa (also of our laboratory) for his helpful comments on the experimentation and on the formulation of this paper.

This work was supported by operating grants to T.J.B. and A.J.C. from the Canadian Bacterial Diseases Network, which is funded as a National Center of Excellence. The electron microscopy was done in the NSERC Guelph Regional STEM Facility, which is partially funded by a National Sciences and Engineering Research Council of Canada infrastructure grant to T.J.B.

REFERENCES

1. **Arsenault, T., D. W. Hughes, D. B. Maclean, W. A. Szarek, A. M. Kropinski, and J. S. Lam.** 1991. Structural studies on the polysaccharide portion of "A-band" lipopolysaccharide from a mutant (AK 1401) of *Pseudomonas aeruginosa* PAO1. Can. J. Chem. **69:**1273–1280.
2. **Bernadsky, G., T. J. Beveridge, and A. J. Clarke.** 1994. Analysis of the sodium dodecyl sulfate-stable peptidoglycan autolysins of select gram-negative pathogens by using renaturing polyacrylamide gel electrophoresis. J. Bacteriol. **176:**5225–5232.
3. **Berry, D., and A. M. Kropinski.** 1986. Effect of lipopolysaccharide mutations and temperature on plasmid transformation efficiency in *Pseudomonas aeruginosa*. Can. J. Microbiol. **32:**436–438.
4. **Beveridge, T. J.** 1989. The structure of bacteria, p. 1–65. *In* J. S. Poindexter and E. R. Leadbetter (ed.), Bacteria in nature, vol. 3. Plenum Publishing Corp., New York.
5. **Díaz, E., E. García, C. Ascaso, E. Méndez, R. López, and J. L. García.** 1989. Subcellular localization of the major pneumococcal autolysin: a peculiar mechanism of secretion in *Escherichia coli*. J. Biol. Chem. **264:**1238–1244.
6. **Ehlert, K., J.-V. Höltje, and M. F. Templin.** 1995. Cloning and expression of a murein hydrolase lipoprotein from *Escherichia coli*. Mol. Microbiol. **16:** 761–768.
7. **Gilleland, H. E., Jr., and R. G. E. Murray.** 1975. Demonstration of cell division by septation in a variety of gram-negative rods. J. Bacteriol. **121:** 721–725.
8. **Graham, L. L., and T. J. Beveridge.** 1990. Effect of chemical fixatives on accurate preservation of *Escherichia coli* and *Bacillus subtilis* structure in cells prepared by freeze-substitution. J. Bacteriol. **172:**2150–2157.
9. **Helmstetter, C. E.** 1987. Timing of synthetic activities in the cell cycle, p. 1594–1605. *In* F. C. Neidhardt, J. L. Ingraham, K. B. Low, B. Magasanik, M. Schaechter, and H. E. Umbarger (ed.), *Escherichia coli* and *Salmonella typhimurium*: cellular and molecular biology. American Society for Microbiology, Washington, D.C.
10. **Helmstetter, C. E., C. Eenhuis, P. Theisen, J. Grimwade, and L. C. Leonard.** 1992. Improved bacterial baby machine: application to *Escherichia coli* K-12. J. Bacteriol. **174:**3445–3449.
11. **Hobot, J. A., and H. J. Rogers.** 1991. Intracellular location of the autolytic *N*-acetylmuramyl-L-alanine amidase in *Bacillus subtilis* 168 and in an autolysis-deficient mutant by immunoelectron microscopy. J. Bacteriol. **173:**961–967.
12. **Höltje, J.-V., and E. I. Tuomanen.** 1991. The murein hydrolase of *Escherichia coli*: properties, functions and impact on the course of infections *in vivo*. J. Gen. Microbiol. **137:**441–454.
13. **Hoyle, B. D., and T. J. Beveridge.** 1984. Metal binding by the peptidoglycan sacculus of *Escherichia coli* K-12. Can. J. Microbiol. **30:**204–211.
14. **Kadurugamuwa, J. L., and T. J. Beveridge.** 1995. Virulence factors are released from *Pseudomonas aeruginosa* in association with membrane vesi-

cles during normal growth and exposure to gentamicin: a novel mechanism of enzyme secretion. J. Bacteriol. **177:**3998–4008.
15. **Kadurugamuwa, J. L., and T. J. Beveridge.** 1996. Bacteriolytic effect of membrane vesicles from *Pseudomonas aeruginosa* on other bacteria including pathogens: conceptually new antibiotics. J. Bacteriol., in press.
16. **Kadurugamuwa, J. L., A. J. Clarke, and T. J. Beveridge.** 1993. Surface action of gentamicin on *Pseudomonas aeruginosa*. J. Bacteriol. **175:**5798–5805.
17. **Kadurugamuwa, J. L., J. S. Lam, and T. J. Beveridge.** 1993. Interaction of gentamicin with the A-band and B-band lipopolysaccharides of *Pseudomonas aeruginosa* and its possible lethal effect. Antimicrob. Agents Chemother. **37:**715–721.
18. **Knirel, Y. A., E. V. Vinogradov, N. A. Kocharova, N. A. Paramonov, N. K. Kochetkov, B. A. Dmitriev, E. S. Stanislavsky, and B. Lanyi.** 1988. The structure of O-specific polysaccharides and serological classification of *Pseudomonas aeruginosa*. Acta Microbiol. Hung. **35:**3–24.
19. **Koch, A. L.** 1990. Additional arguments for the key role of "smart" autolysins in the enlargement of the wall of gram-negative bacteria. Res. Microbiol. **141:**529–541.
20. **Koike, M., K. Iida, and T. Matsuo.** 1969. Electron microscopic studies on the mode of action of polymyxin. J. Bacteriol. **97:**448–452.
21. **Laemmli, U. K.** 1970. Cleavage of structural proteins during the assembly of the head of bacteriophage T4. Nature (London) **227:**680–685.
22. **Lam, J. S., L. L. Graham, J. Lightfoot, T. Dasgupta, and T. J. Beveridge.** 1992. Ultrastructural examination of lipopolysaccharides of *Pseudomonas aeruginosa* strains and their isogenic rough mutants by freeze-substitution. J. Bacteriol. **174:**7159–7167.
23. **Lightfoot, J., and J. S. Lam.** 1991. Molecular cloning of genes involved with expression of A-band lipopolysaccharide, an antigenically conserved form, in *Pseudomonas aeruginosa*. J. Bacteriol. **173:**5624–5630.
24. **Martin, N. L., and T. J. Beveridge.** 1986. Gentamicin interaction with *Pseudomonas aeruginosa*. Antimicrob. Agents Chemother. **29:**1079–1087.
25. **Rivera, M., L. E. Bryan, R. E. W. Hancock, and E. J. McGroarty.** 1988. Heterogeneity of lipopolysaccharides from *Pseudomonas aeruginosa*: analysis of lipopolysaccharide chain length. J. Bacteriol. **170:**512–521.
26. **Rivera, M., and E. J. McGroarty.** 1989. Analysis of a common antigen lipopolysaccharide from *Pseudomonas aeruginosa*. J. Bacteriol. **171:**2244–2248.
27. **Rogers, H. J., H. R. Perkins, and J. B. Ward.** 1980. The bacterial autolysins, p. 437–460. *In* H. J. Rogers, H. R. Perkins, and J. B. Ward (ed.), Microbial cell walls and membranes. Chapman & Hall, Ltd., London.
28. **Ronda, C., J. L. García, E. García, J. M. Sánchez-Puelles, and R. López.** 1987. Biological role of the pneumococcal amidase: cloning of the *lytA* gene in *Streptococcus pneumoniae*. Eur. J. Biochem. **164:**621–624.
29. **Schleifer, K. H., and O. Kandler.** 1972. Peptidoglycan types of bacterial cell walls and their taxonomic implications. Bacteriol. Rev. **36:**407–471.
30. **Shockman, G. D., and J.-V. Höltje.** 1994. Microbial peptidoglycan (murein) hydrolases, p. 131–166. *In* J.-M. Ghuysen and R. Hakenbeck (ed.), Bacterial cell wall. Elsevier, Amsterdam.
31. **Smith, T. J., and S. J. Foster.** 1995. Characterization of the involvement of two compensatory autolysins in mother cell lysis during sporulation of *Bacillus subtilis* 168. J. Bacteriol. **177:**3855–3862.
32. **Tomasz, A.** 1983. Murein hydrolases—enzymes in search of a physiological function, p. 155–172. *In* R. Hakenbeck, J.-V. Höltje, and H. Labischinski (ed.), The target of penicillin. Walter de Gruyter & Co., Berlin.
33. **Towbin, H., T. Staehelin, and J. Gordon.** 1979. Electrophoretic transfer of proteins from polyacrylamide gels to nitrocellulose sheets: procedure and some applications. Proc. Natl. Acad. Sci. USA **76:**4350–4354.
34. **Walderich, B., and J.-V. Höltje.** 1991. Subcellular distribution of the soluble lytic transglycosylase in *Escherichia coli*. J. Bacteriol. **173:**5668–5676.
35. **Walker, S. G., and T. J. Beveridge.** 1988. Amikacin disrupts the cell envelope of *Pseudomonas aeruginosa* ATCC 9027. Can. J. Microbiol. **34:**12–18.
36. **Watt, S. R., and A. J. Clarke.** 1994. Initial characterization of two extracellular autolysins from *Pseudomonas aeruginosa* PAO1. J. Bacteriol. **176:**4784–4789.
37. **Wilkinson, S. G.** 1983. Composition and structure of lipopolysaccharides from *Pseudomonas aeruginosa*. Rev. Infect. Dis. **5:**S941–S949.